Anal. Bioanal. Electrochem., Vol. 15, No. 6, 2023, 506-515
https://www.doi.org/10.22034/abec.2023.705729

Analytical & Bioanalytical Electrochemistry

Full Paper

New Synthesis and Characterization of $NiMoO_4/Mn(VO_3)_2$ Heterostructures for Electrochemical Detection of Dopamine

Ali Sobhani-Nasab,[1,*] Amir Ghaderi,[2,3,*] Hamid Reza Banafshe,[1] Mostafa Bakhshi-kashi,[4] Esmaeil Sohooli,[5] Reza Eshraghi,[1] Amin Moradi Hasan-Abad,[6] and Mehdi Rahimi-Nasrabadi[7,8]

[1]*Physiology Research Center, Institute for Basic Sciences, Kashan University of Medical Sciences, Kashan, Iran*
[2]*Department of Addiction Studies, School of Medicine, Kashan University of Medical Sciences, Kashan, Iran*
[3]*Clinical Research Development Unit-Matini/Kargarnejad Hospital, Kashan University of Medical Sciences, Kashan, Iran*
[4]*Student Research Committee, Kashan University of Medical Sciences, Kashan, Iran*
[5]*Department of Chemistry, Faculty of Science, Electrochemical Sensors Research Laboratory, Shahid Rajaee Teacher Training University, Lavizan, P.O. Box 1678815811, Tehran, Iran*
[6]*Autoimmune Diseases Research Center, Shahid Beheshti Hospital, Kashan University of Medical Sciences, Kashan, Iran*
[7]*Institute of Electronic and Sensor Materials, TU Bergakademie Freiberg, Freiberg 09599, Germany*
[8]*Chemical Injuries Research Center, Systems Biology and Poisonings Institute, Baqiyatallah University of Medical Sciences, Tehran, Iran*

*Corresponding Author, Tel.: +989137290874
E-Mails: Ali.sobhaninasab@gmail.com ; Gaderiam@yahoo.com

Received: 27 April 2023 / Received in revised form: 18 June 2023 / Accepted: 21 June 2023 / Published online: 30 June 2023

Abstract- The goal of this study is to establish a simple and convenient co-precipitation approach for the ultrasonic synthesis of $NiMoO_4/Mn(VO_3)_2$ heterostructures without capping agents and to adapt the glassy carbon electrode with this material for electrochemical detection of dopamine. To analyze the chemical structure and morphology of nanostructures, field emission scanning electron microscopy (FE-SEM) and X-ray diffraction (XRD) techniques were used. The ultrasonic wave for pure NiMoO4/$Mn(VO_3)_2$ heterostructures with

homogeneous sphere-like shape and small particle size around 30-40 nm was discovered using FESEM and XRD results. Electrochemical sensors have been sought after for studying biological, environmental, and pharmaceutical species due to their long-term reliability, high sensitivity, and accuracy, as well as their low cost, speed, and ease of shrinking. Differential pulse voltammetry (DPV) and cyclic voltammetry (CV) were used to conduct electrochemical experiments of the GCE/$NiMoO_4$/$Mn(VO_3)_2$ towards dopamine (DA) detection. According to the DPV results, the modified sensor revealed a linear concentration range of 1 to 60 μM with a limit of detection of 0.33 M and high selectivity.

Keywords- $NiMoO_4$/$Mn(VO_3)_2$; Heterostructures; Dopamine; Electrochemical sensing; Co-precipitation method

1. INTRODUCTION

The intriguing size-dependent optical, mechanical, magnetic, chemical, electrical, and thermal properties of one-dimensional inorganic luminous nanomaterials such as nanotubes, nanowires, nanofibers, nanobelts, and nanorods are of fundamental importance. They see potential applications in molecular computing, nanomedicine, energy storage, fuel cells, sensors, and tunable resonant devices from this standpoint [1-6].

Due to their interesting size-dependent optical, mechanical, thermal, electrical, magnetic, and chemical properties, one-dimensional inorganic luminous nanomaterials like nanofibers, nanobelts, nanowires, and nanorods, are of fundamental interest. As a result, they see potential uses for their technology in fuel cells, energy storage, molecular computing, nanomedicine, tunable resonant devices, sensors, and nanophotonics [7-9].

The long-term dependability, high sensitivity, and accuracy of electrochemical sensors, as well as their affordability, speed, and simplicity of scaling, have made them useful for studying biological, environmental, industrial, and pharmaceutical species [10-17]. Numerous exceptional nanomaterials, including metal oxides, metals, metal-organic, carbon-based nanomaterial frameworks and conductive polymers have been used for electrochemical assays for more than 20 years to improve analytical performance [18-21]. A neurochemical transmitter to the brain called dopamine (DA), was identified by Arvid Carlsson in 1957 [22]. The cardiovascular, central nervous system, endocrinology, and renal systems are all impacted by dopamine. DA also keeps track of a number of bodily processes, including cognition, movement, mood, behavior, learning, and attention [23-26]. Depression, addiction, schizophrenia, and neurodegenerative conditions like Alzheimer's and Parkinson's may all be brought on by an imbalance in DA levels in the human brain [27]. Alzheimer's, Parkinson's, addiction, and other neurodegenerative conditions can all be brought on by an imbalance in DA levels in the human brain. Several techniques, including chemiluminescence, chromatographic, colorimetric, fluorescence, and spectrophotometry, are used to determine the DA [28-30]. These conventional techniques also need expensive and time-consuming sample pretreatments that are tedious [31,32]. Therefore, it is essential to employ techniques that have the following characteristics: quick response time, low cost, simplicity, low detection limit,

selectivity, and high sensitivity [1,33,34]. Our goal is to create $NiMoO_4/Mn(VO_3)_2$ heterostructures for the electrochemical detection of DA using these precursors: $Ni(NO_3)_2.H_2O$, $Mn(NO_3)_2.6H_2O$, NH_4VO_3, and $(NH_4)6Mo_7O_{24}$.

2. EXPERIMENTAL SECTION

2.1. Materials and characterization

In this experiment, all of the chemical reagents were of analytical quality and were utilized directly. A Philips-X'PertPro X-ray diffractometer was used to record the X-ray diffraction (XRD) patterns while emitting Ni-filtered Cu K radiation with a scan range of 10280. Images from scanning electron microscopy (SEM) using the energy dispersive X-ray spectroscopy on the LEO-1455VP were obtained. Using a Philips XL30 microscope, the energy dispersive spectrometry (EDS) analysis was examined. Shimadzu UV-Vis scanning spectrometer was used to conduct an investigation of UV-Vis diffuse reflectance spectroscopy. At room temperature, the sample's magnetic properties were measured using a vibrating sample magnetometer (VSM) made by Meghnatis Daghigh Kavir Co. in Kashan, Iran.

2.2. Synthesis of $NiMoO_4$ nanoparticles

Separately, 40 ml of distilled water was used to dissolve $Ni(NO_3)_2.H_2O$ (1 mmol) and $(NH_4)_6Mo_7O_{24}$ (2 mmol). Then, while stirring and without adjusting the pH, $(NH_4)_6Mo_7O_{24}$ solution and $Ni(NO_3)_2.H_2O$ solution were combined. The finished product of the reaction was centrifuged, several times washed with ethanol and distilled water, and then dried for 90 minutes at 50 °C in air in a typical furnace.

2.3. Synthesis of $NiMoO_4/Mn(VO_3)_2$ heterostructures

On the basis of earlier research, $NiMoO_4$ nanocrystals were first created. After that, 80 mg of it was ultrasonically mixed with 30 ml of water for 30 minutes. Then, under stirring, a solution of 1 mmol of $Mn(NO_3)_2.6H_2O$ and a solution of 2 mmol of NH_4VO_3 were added to the dispersed $NiMoO_4$ solution. The final precipitate was successively dried, calcined at 500 °C for an hour, and washed three times with distilled water.

2.4. Electrochemical study

An Autolab potentiostat/galvanostat model PGSTAT302 (EcoChemie, Netherlands) was used to conduct electrochemical studies such as cyclic voltammetry (CV) and differential pulse voltammetry (DPV). A three-electrode system was used for all electrochemical experiments. It consisted of a platinum plate as the counter electrode, an Ag/AgCl reference electrode, and GCE/$NiMoO_4/Mn(VO_3)_2$ as the working electrode, which was prepared by drop casting 3 L of

$NiMoO_4/Mn(VO_3)_2$ suspension (1 mg/ml in DMF). Every experiment was conducted at room temperature.

3. RESULTS AND DISCUSSION

3.1 Structural characterization of $NiMoO_4/Mn(VO_3)_2$ heterostructures

Figure 1 displays the XRD patterns of the heterostructures of $NiMoO_4$ and $Mn(VO_3)_2$. Our findings imply that every constructed heterostructure is pure and contains two phases. The first is the tetragonal phase of $NiMoO_4$ and $Mn(VO_3)_2$ (JCPDS 016-0291), while the second is monoclinic (JCPDS 36-0166) with an I41/a space group, respectively. The crystallite diameter (Dc) of $NiMoO_4/Mn(VO_3)_2$ heterostructures is calculated to be 25.3 nm from XRD data and the Scherrer equation ($D_c = K\lambda/\beta\cos\theta$), respectively [28].

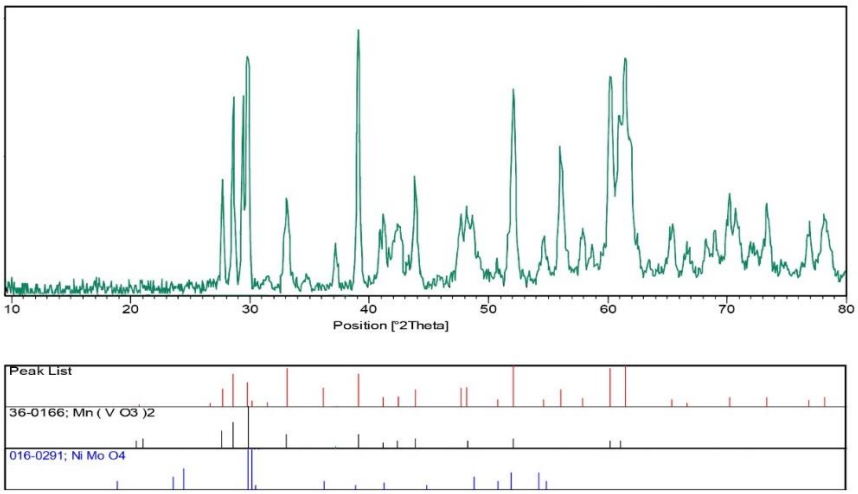

Figure 1. XRD patterns of $NiMoO_4/Mn(VO_3)_2$ heterostructures obtained at 25 °C

FE-SEM was used to examine the morphology of the $NiMoO_4/Mn(VO_3)_2$ heterostructures. Figure 2 shows spherically shaped uniform nanoparticles with an average particle size of about 30-35 nm that are evenly dispersed throughout the sample.

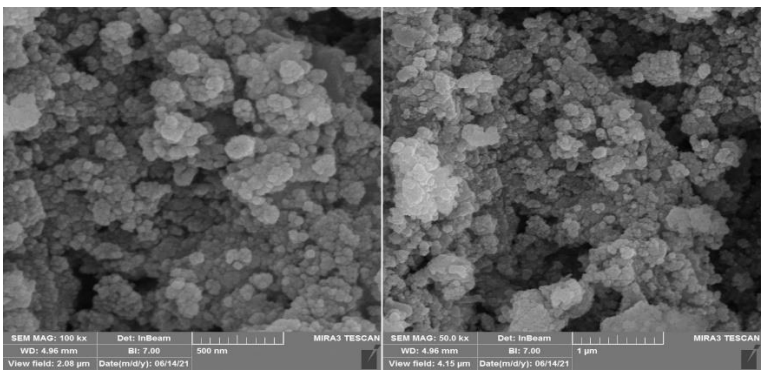

Figure 2. FESEM images of $NiMoO_4/Mn(VO_3)_2$ heterostructures obtained at 25 °C

3.2. Study of the electrochemical behavior of prepared electrodes

To assess the effectiveness of the GCE and GCE/$NiMoO_4$/$Mn(VO_3)_2$ in the electrochemical detection of DA, a cyclic voltammetry technique was created. For this, the CV technique was used at a scan rate of 50 mVs^{-1} with a potential range of -0.1 to 0.5 V in a solution of 50.0 mol L^{-1} DA in 0.1 mol L^{-1} PBS (pH 5.0). Figure 3 shows that the cyclic voltammograms of the two electrodes exhibit a reversible oxidation/reduction peak over the voltage window (-0.1 to 0.5 V). Starting at 0.38 V *vs.* Ag/AgCl, the GCE/ $NiMoO_4$/$Mn(VO_3)_2$ modified electrode exhibits a sizable oxidation current. On the bare GCE and the GCE/ $NiMoO_4$/$Mn(VO_3)_2$, the Ep linked to DA is 0.19 and 0.16 V, respectively (see Figure 3). The modified electrode's increased peak current and decreased difference between its oxidation peak potential and reduction peak potential (E_p) show that electron transfer took place effectively at its surface. A notable capacity to expand the electroactive surface area as well as an enhancement of the electron-transfer between the electrode and the analyte on modified electrode are both shown by a little negative shift of the onset potential for electrooxidation of DA and a considerable amplification of DA peak current. These findings suggest that the redesigned electrode performs more effectively for electrochemical sensing.

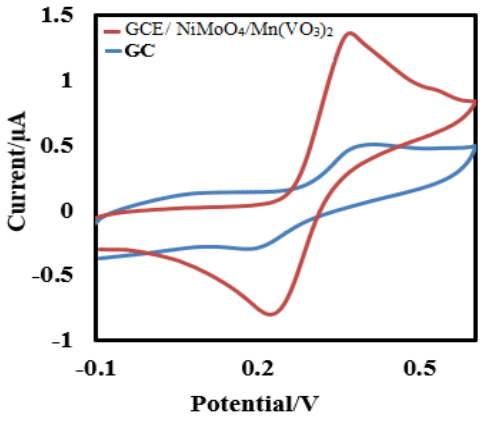

Figure 3. Cyclic voltammetry of the surface of the GCE and GCE/ $NiMoO_4$/$Mn(VO_3)_2$ in 50.0 µmol L^{-1} DA in 0.1 mol L^{-1} PBS (pH 5.0)

CV was used to examine the kinetic behavior of DA over the GCE/$NiMoO_4$/$Mn(VO_3)_2$ fabricated surface as well as the electrochemical mechanism of electrode reaction. The built electrode's acquired voltammograms in 0.l M PB solution (pH 5) containing 50.0 mol L^{-1} at various scan rates ranging from 30 to 200 mVs^{-1} are shown in Figure 4. The rise in cathodic peak current caused by raising the scan rate from 30 to 200 mVs^{-1} is clearly shown in Figure 4A. The square root of the scan rate has an agreeable linear association with the decrease peak current (I_{pc}). The square root of the scan rate is shown against the cathodic peak currents for electro-oxidation of DA in Figure 4B, and its linear regression equation is stated as: y= 0.17x-0.24 and y=-0.11x+0.10, indicating that at the interface between the target species' DA-

containing electrolyte and electrode system, the diffusion process regulates the acquired current amplitude data.

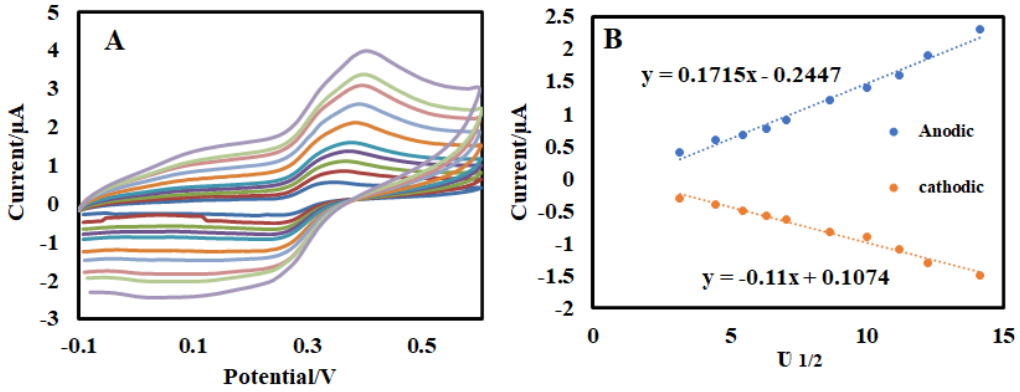

Figure 4. (A) Effect of the scan rate on cyclic voltammograms response of 50.0 µmol L^{-1} DA (pH=5) at GCE/ $NiMoO_4/Mn(VO_3)_2$ electrode with different scan rates (30-200 mVs^{-1}) and (B) Dependency of the peak currents to square root of the scan rate

At GCE/$NiMoO_4/Mn(VO_3)_2$, cyclic voltammetry experiments were carried out to examine the impact of pH (3.0-7.0) on I_p and E_p of DA. According to Figure 5, the largest peak current is visible at pH 5.0 (green curve), which was chosen for the studies that followed. In Figure 5, the link between E_p and pH is also depicted. Peak potential changes downward as pH rises, as evidenced by the equation of the straight-line Y = -0.069X+0.697, (r^2 = 0.994). The slope of E_p vs. pH is -0.069 V pH^{-1}, which is close to the theoretical value of -0.059 V pH^{-1}, indicating that the electro-reduction of DA involved an equal number of protons and electrons.

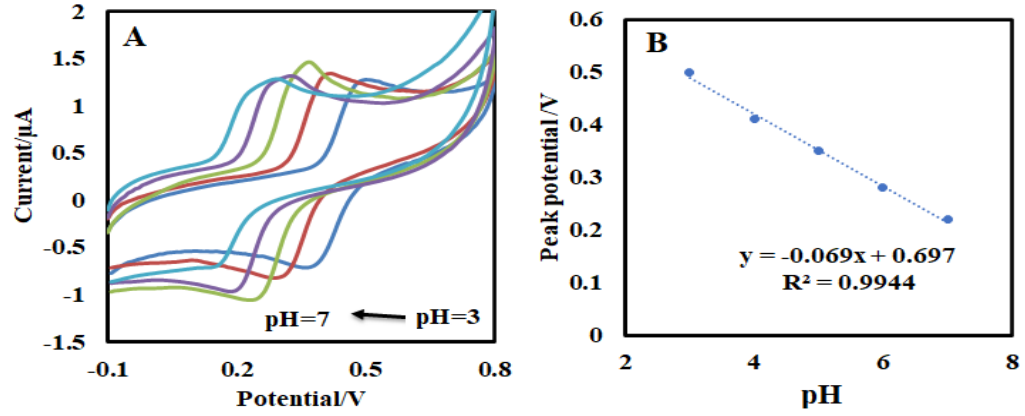

Figure 5. (A) Influence of pH on the reduction peak current and (B) potential of CV for of 50.0 µmol L^{-1} DA at the GCE/ $NiMoO_4/Mn(VO_3)_2$

Using the DPV approach, GCE/$NiMoO_4/Mn(VO_3)_2$ were quantified at various DA concentrations on GCE/ $NiMoO_4/Mn(VO_3)_2$ in the presence of 0.05 M PBS (pH 5.0) under

optimal voltammetric conditions, as shown in Figure 6. In the concentration range of the DA from 1 to 60 µM, it is evident that the peak current versus the DA concentration has a linear connection with a slope of 0.0208 A M^{-1} (equation regression y=0.0208x+0.1349 with R^2=0.994). Additionally, the following methods can be used to establish the low limit of detection (LOD) and limit of quantification (LOQ) of LOD [35,36]:

LOD=3K/∂

LOQ=10K/∂

where, ∂ = corresponding to the linear slope and k = standard deviation method from the detected blank solution of three measurements. The first linear plot of $NiMoO_4/Mn(VO_3)_2$/GCE shows a low LOD of 0.33 µM and LOQ of 1 µM, respectively, using the aforementioned equations. The sensor has a wide linear range, decreased LOD, and good sensitivity (seen through the calibration curve's slope), all of which can be attributed to the modified electrode's enhanced effective surface area.

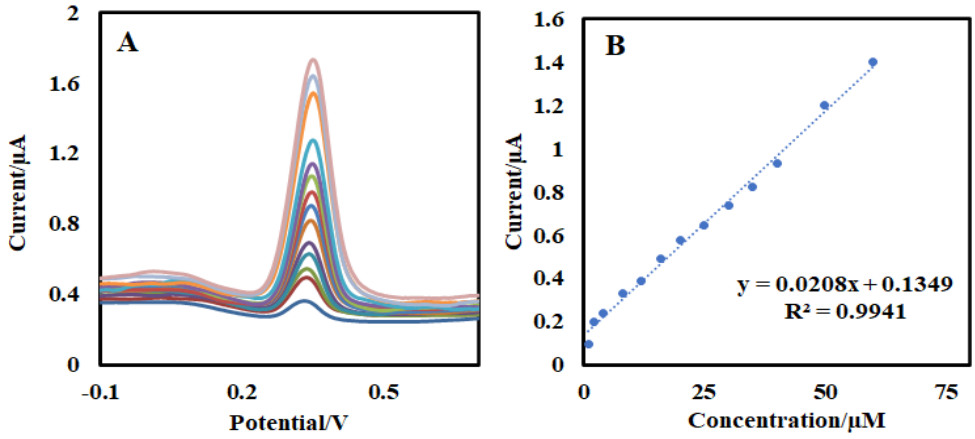

Figure 6. The recorded differential pulse voltammograms for v concentrations of DA from 1-60 µM on the GCE/ $NiMoO_4/Mn(VO_3)_2$ in PB with pH= 5 and (B) relative calibration curve

Using GCE/$NiMoO_4/Mn(VO_3)_2$ in PBS (pH=5.0) containing 15 µM of DA in the presence of Cl^-, Na^+, K^+, Mg^{2+} and SO_4^{2-} (1 mM), as well as glucose, caffeine, and ascorbic acid (100 µM), the selectivity of the sensor was examined using the DPV approach towards DA. The original peak, where the change in signals due to interference was less than 4%, is unaffected by the presence of 1 mM interfering species in the presence of 15 µM DA. The findings demonstrated that the addition of interfering species had no discernible impact on the I_{pc} current and E_{pc} potential of 15 µM DA. The modified electrode was shown to have high selectivity performance for the detection of DA without altering cross-interfering species.

The suggested sensor's applicability was evaluated by measuring the amount of DA in a sample of human serum at the surface of a GCE/$NiMoO_4/Mn(VO_3)_2$ electrode. The samples were made using the conventional addition procedure (Table 1). In these assays, no DA at all was found in

serum samples from healthy people. By obtaining the recovery of known amounts of DA spiked in the serum solutions at various concentrations, the accuracy of the analysis was assessed. The results demonstrate an average recovery of 93% and 96.5% for DA given to the serum samples, respectively, demonstrating the method's dependably accurate performance.

Table 1. Analysis of human serum sample by differential pulse voltammetry on the GCE/ $NiMoO_4/Mn(VO_3)_2$

Sample	Target	Detected (μM)	Added (μM)	Found (μM)	Recovery (%)	RSD (n = 3) (%)
Serum (I)	DA	-	10	9.3	93	3.42
Serum (II)	DA	-	20	19.3	96.5	2.92

4. CONCLUSION

In conclusion, a simple method for creating heterostructures of $NiMoO_4$ and $Mn(VO_3)_2$ is disclosed. In addition, the synthetic substance was applied to the glassy carbon electrode to change it for the electrochemical detection of DA. By using XRD and SEM to analyze the morphology and particle size of the finished goods, as well as CV and DPV to study electrochemical research. The suggested sensor was based on modifying the GCE using straightforward, inexpensive materials, and it demonstrated a vibrant concentration-dependent signal throughout a broad linear response range for the determination of the DA between 1 and 60 μM with a limit of detection of 0.33 μM and excellent selectivity. These results show that the proposed improved material can be used for additional electrocatalysis fields as well as the electrochemical detection of DA.

Acknowledgement

The Kashan University of Medical Sciences (kums) (Grant No. 98110) (IR.KAUMS.MEDNT.REC.1398.074) is gratefully acknowledged by the authors for its assistance.

REFERENCES

[1] A. Moradi Hasan-Abad, M.A. Esmaili, M. Akbari, A.M. Sorouri, L. Hosseinzadeh, and A. Anal. Bioanal. Electrochem. 14 (2022) 1152.

[2] M. Akbari, M.S. Mohammadnia, M. Ghalkhani, M. Aghaei, E. Sohouli, M. Rahimi-Nasrabadi, M. Arbabi, H.R. Banafshe, and A. Sobhani-Nasab, J. Industrial Eng. Chem. 114 (2022) 418.

[3] M. Ghalkhani, E.M. Khosrowshahi, E. Sohouli, K. Eskandari, M. Aghaei, M. Rahimi-Nasrabadi, A. Sobhani-Nasab, H. Banafshe, and E. Kouchaki, Surfaces and Interfaces 30 (2022) 101943.

[4] H. Halakoei, M. Ghalkhani, A. Sobhani-Nasab, and M. Rahimi-Nasrabadi, Mater. Res. Express 8 (2021) 085001.

[5] H.R. Naderi, A. Sobhani-Nasab, E. Sohouli, K. Adib, and E. Naghian, Anal. Bioanal. Electrochem. 12 (2020) 263.

[6] H. Naderi, H. Sobati, A. Sobhani-Nasab, M. Rahimi-Nasrabadi, M. Eghbali-Arani, M.R. Ganjali, and H. Ehrlich, ChemistrySelect, 4 (2019) 2862.

[7] A. Sobhani-Nasab, S. Pourmasoud, F. Ahmadi, M. Wysokowski, T. Jesionowski, H. Ehrlich, and M. Rahimi-Nasrabadi, Mater. Lett. 238 (2019) 159.

[8] M. Eghbali-Arani, S. Pourmasoud, F. Ahmadi, M. Rahimi-Nasrabadi, V. Ameri, and A. Sobhani-Nasab, Arabian J. Chem. 13 (2020) 2425.

[9] S. Behvandi, A. Sobhani-Nasab, M.A. Karimi, E. Sohouli, M. Karimi, M.R. Ganjali, F. Ahmadi, and M. Rahimi-Nasrabadi, Polyhedron 180 (2020) 114424.

[10] P. Norouzi, G.R.N. Bidhendi, M.R. Ganjali, A. Sepehri, M. Ghorbani, Microchim. Acta 152 (2005) 123.

[11] P. Norouzi, M.R. Ganjali, and L. Hajiaghababaei, Anal. Lett. 39 (2006) 1941.

[12] V. Arabali, M. Ebrahimi, M. Abbasghorbani, V.K. Gupta, M. Farsi, M.R. Ganjali, and F. Karimi, J. Mol. Liq. 213 (2016) 312.

[13] P. Norouzi, M.R. Ganjali, and P. Matloobi, Electrochem. Commun. 7 (2005) 333.

[14] H. Beitollahi, Z. Dourandish, S. Tajik, M.R. Ganjali, P. Norouzi, and F. Faridbod, J. Rare Earth 36 (2018) 750.

[15] P. Norouzi, F. Faridbod, B. Larijani, and M.R. Ganjali, Int. J. Electrochem. Sci. 5 (2010) 1213.

[16] M.R. Ganjali, H. Beitollahi, R. Zaimbashi, S. Tajik, M. Rezapour, and B. Larijani, Int. J. Electrochem. Sci. 13 (2018) 2519.

[17] P. Norouzi, M.R. Ganjali, A. Sepehri, and M. Ghorbani, Sens. Actuator B 110 (2005) 239.

[18] A. Khoobi, F. Shahdost-fard, M. Arbabi, M. Akbari, H. Mirzaei, M. Nejati, M. Lotfinia, A. Sobhani-Nasab, and H.R. Banafshe, Polyhedron 177 (2020) 114302.

[19] M.H. Ghanbari, F. Shahdost-Fard, M. Rostami, A. Khoshroo, A. Sobhani-Nasab, N. Gholipour, H. Salehzadeh, M.R. Ganjali, M. Rahimi-Nasrabadi, and F. Ahmadi, Microchim. Acta 186 (2019) 1.

[20] A. Khoshroo, L. Hosseinzadeh, A. Sobhani-Nasab, M. Rahimi-Nasrabadi, and F. Ahmadi, Microchem. J. 145 (2019) 1185.

[21] A. Moradi Hasan-Abad, M.A. Esmaili, A. Ghotaslou, A. Atapour, A. Khoshroo, and E. Naghian, Anal. Bioanal. Electrochem. 14 (2022) 1060.

[22] V.K. Yeragani, M. Tancer, P. Chokka, and G.B. Baker, Indian Journal of Psychiatry 52 (2010) 87.
[23] D. Kim, S. Lee, and Y. Piao, J. Electroanal. Chem. 794 (2017) 221.
[24] H.W. Yu, J.h. Jiang, Z. Zhang, G.C. Wan, Z.Y. Liu, D. Chang, H.Z. Pan, Anal. Biochem. 519 (2017) 92.
[25] J. Fang, Z. Xie, G. Wallace, and X. Wang, Applied Surface Sci. 412 (2017) 131.
[26] A.M. Hasan-Abad, E. Adabi, E. Sadroddiny, M.R. Khorramizadeh, M.A. Mazlomi, S. Mehravar, and G.A. Kardar, Iranian Journal of Allergy, Asthma and Immunology (2019) 427.
[27] V. Sharma, A. Sundaramurthy, A. Tiwari, and A.K. Sundramoorthy, Applied Surface Sci. 449 (2018) 558.
[28] L.Q. Xie, Y.H. Zhang, F. Gao, Q.A. Wu, P.Y. Xu, S.S. Wang, N.N. Gao, and Q.X. Wang, Chinese Chem. Lett. 28 (2017) 41.
[29] P. Wiench, Z. González, R. Menéndez, B. Grzyb, and G. Gryglewicz, Sens. Actuators B 257 (2018) 143.
[30] A. Ejaz, Y. Joo, and S. Jeon, Sens. Actuators B 240 (2017) 297.
[31] Y. Haldorai, A.E. Vilian, M. Rethinasabapathy, Y.S. Huh, and Y.K. Han, Sens. Actuators B 247 (2017) 61.
[32] X. Liu, E. Shangguan, J. Li, S. Ning, L. Guo, and Q. Li, Mater. Sci. Eng. C 70 (2017) 628.
[33] Y. Li, Y. Gu, B. Zheng, L. Luo, C. Li, X. Yan, T. Zhang, N. Lu, and Z. Zhang, Talanta 162 (2017) 80.
[34] A.E. Vilian, S. An, S.R. Choe, C.H. Kwak, Y.S. Huh, J. Lee, and Y.K. Han, Biosens. Bioelectron. 86 (2016) 122.
[35] M. Nouri, M. Rahimnejad, G. Najafpour, and A.A. Moghadamnia, ChemistrySelect 4 (2019) 13421.
[36] G. Kesavan, V. Vinothkumar, and S.M. Chen, Journal of Alloys and Compounds 867 (2021) 159019.